COMPUTATIONAL RESEARCH PROGRESS IN APPLIED SCIENCE & ENGINEERING (CRPASE)

CRPASE: TRANSACTIONS OF CIVIL AND ENVIRONMENTAL ENGINEERING

Journal homepage: http://www.crpase.com

CRPASE: Transactions of Civil and Environmental Engineering 8 (1) Article ID: 2746, 1–10, March 2022 ISSN 2423-4591

Research Article

Smart Window Design Tool: Daylight Transmission by Using Transparent Color Filters

Bahar Sultan Qurraie *

Faculty of Architecture, Karabük University, Karabük, Turkey

Keywords

Radiation Transmission,
Smart Window Design Tool,
Cooling Load,
Color Filters,
MATLAB,
Light Transmittance.

Abstract

In hot climates, the work carried out has a significant share in reducing cooling loads within the scope of increasing energy efficiency in the buildings that are dependent on foreign energy supply. Based on stained glasses, this study has developed a program that allows glass surfaces to be designed with colored glasses depending on light transmission, absorption and reflection characteristics of different colors in accordance with the needs of the space as well as for use on facades with large glass surfaces that are exposed to the sun. The aim of this study is to find a multi-functional window designing system without considering the glass material. The colored transparent polymers are designed as the moving shaded elements placed on the window as window blinds. MATLAB is used in this study to write the program according to the climate data. The color, number of blinds and window prototypes are found by placing the data obtained through the laboratory studies of polymers in this software. Decreasing irradiance transmission in summer especially in A and B climate classifications is found to be important as the results show that the green and blue transparent filters transmit a minimum of 22 percent. The window prototypes are designed as two rows of blinds according to the window and the zone where they are located and placed in double or triple glazed windows. The simulation results of the Smart Window Design Tool (SWDT) can be shifted to any window geometry by defining the two season types.

1. Introduction

The amount of energy consumed to ensure the comfort conditions in sustainable buildings corresponds to 40% of total energy consumption [4-6]. One of the most fundamental problems concerning today's architecture is to prevent excessive heat gain of large glass facades exposed to sun and reduce the cooling loads [7-10]. Among different methods used, the colored glasses can be considered as an alternative to avoid this problem. As a method, the colors can be used depending on their characteristics having different transmission percent of spectra in different wavelengths [11,12]. This study focuses on preventing undesirable sunlight during summer months, ensuring sufficient natural lighting for indoor comfort conditions, and developing a model to minimize the energy consumed for cooling by avoiding excessive radiation. Therefore, while developing this program, it was necessary to evaluate the wavelength

* Corresponding Author: Bahar Sultan Qurraie
E-mail address: Baharsultan@karabuk.edu.tr, ORCID: https://orcid.org/0000-0002-5142-3367

Received: 23 December 2021; Revised: 8 March 2022; Accepted: 10 March 2022
https://doi.org/10.52547/crpase.8.1.2746

Academic Editor: **Vahid Najafi Moghadam Gilani**

Please cite this article as: B. S. Qurraie, Smart Window Design Tool: Daylight Transmission by Using Transparent Color Filters, Computational Research Progress in Applied Science & Engineering, CRPASE: Transactions of Civil and Environmental Engineering 8 (2022) 1–10, Article ID: 2746.

properties of colors first. In this respect, the study was carried out with different aspects.

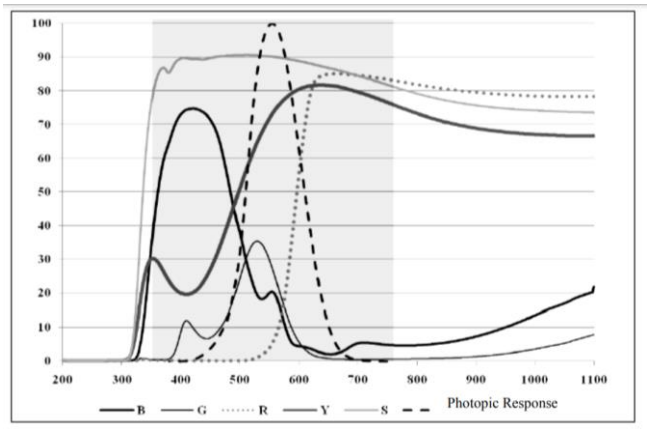

Figure 1. Test results of the transmission spectra obtained from the colored glass [3].

1.1. Literature Review

Transmittance refers to the percentage of radiation that can pass through glazing. Transmittance can be classified in terms of different types of light or energy, e.g., "visible light transmittance," "UV transmittance," or "total solar energy transmittance" [13]. It can transmit electromagnetic waves and also provides access to the sunrays because the glass carries the name of a transparent material. Even most glasses do not pass most of the ultraviolet and infrared waves [14, 15]. The US Department of Energy (DOE) suggests that having spectrally selective capabilities of glasses causes a reduction in the solar load of the building [16].

The architectural glass comes in three different strength categories [17] as "annealed glass, heat-strengthened glass, and fully tempered glass." Stained glass is one of the types of annealed glass. According to [18], stained glass contains minerals that color the glass uniformly through its thickness and promote absorption of visible light and infrared radiation. Different glass types have some other properties for solar radiation [19-22] known to be reflected, transmitted, absorbed, and re-radiated.

In a research on Orosi [23-25] glasses (stained glasses in Iran) in 2006 and 2015 [3, 26], the green, blue, red, and yellow glasses, light visibility, and light passing through long wavelengths were investigated. Accordingly, the results that were seen on the spectrophotometer are given in Figure 1 above.

Glass systems providing dynamic control in high performance facade systems are generally described as "smart glasses". The term "smart" refers to the ability of glass systems to be controlled in response to changing environmental conditions. In passive windows, a multi-layer coating applied to window glass [27-29] or a structure with nanoparticles [14] embedded in a glass matrix can help prevent unwanted transmission of IR radiation [30, 31]. In electrochromic glass systems, it was reported by a few [30, 32-35] that a potential of 1 to 5 volts is applied to the tungsten oxide film layer [36], which is then applied as a multilayer film of about 1 micron thickness. In a study conducted on Electrochromic glass and Low-e glass office windows [37], more workers in office having Low-e glass coating were found to experience eyestrain and headache as compared to workers in the Electrochromic glass buildings. The new window system was organized in such a way to decrease the headache and eyestrain caused by the glass types.

2. Methodology

The MATLAB [38] software program is a comprehensive calculation program, and therefore, it has been used as a basis in this study. There were basic formulas and standards to be used in the program and they were entered using two-dimensional modeling codes [39, 40]. Preventing undesirable sunlight during summer months, ensuring sufficient natural lighting for indoor comfort conditions, and developing a model to minimize the energy consumed for cooling is the basis of the project by avoiding excessive heat gain. The model thus created combines the color glass applications commonly used in the past with the present technology and predicts color features. The color percentages calculated based on the zone, climate, position, and the given window size data will – by the recognized method – be able to provide designers with an opportunity to create different compositions by providing indoor comfort conditions in the context of thermal and lighting without needing test potential on the facades nor another shading element. Since the Smart Window Design Tool (SWDT) is a two-dimensional drawing, the user will be able to enter the window, wall, and zone information more easily. In the program, the two fundamental problems are desired to be solved. The first goal is to avoid losing visual comfort that allows more light to pass through and the second goal is to obtain less heat gain. ASHRAE standards [27], a worldwide standard, have been used to achieve these goals. In this study, the data obtained by using the content analysis method and the experimental research method are tested over and over in the laboratory and computer environment. It can be seen in Figure 2. In order to solve the indemnification problem of research, smart window design tool (SWDT) was modeled in MATLAB.

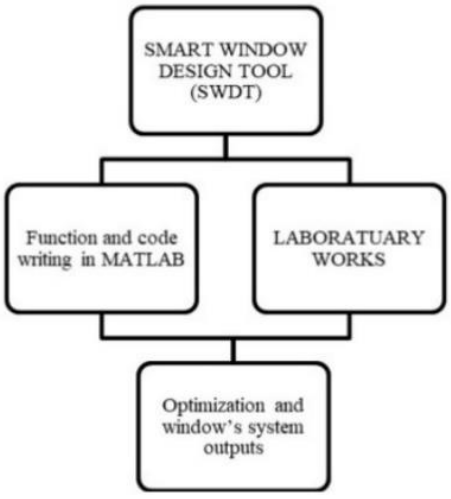

Figure 2. The process diagram of study

The model [41] (Figure 3) combines the stained-glass applications that were commonly used in the past, with the

present technology and predicts color features. Today, based on many factors, fatigue with prolonged atriums can be seen in some people residing in larger structures. The main reason for this is the combination of non-natural products and the radiation generated by electric-magnetic fluxes. This paper aims to reduce this radiation and contribute to cooling energy for the use of nutritional and functional properties of Orosi glasses.

The system consists of a mid-pane shading device between double glazing panes with an external vent on top. The colored transparent filters (CTFs) between these two glasses are placed vertically in two rows of jalousies as vertical blinds, as shown in Figure 3. The system considered is double-glazed having ventilation to outside [42-45]; however, it is expected that the mid-pane shading device in triple-glazed [46-48] top vent can be more responsive.

The programming of SWDT is provided in the MATLAB language and has been coded in two phases. In the first phase, the programming was codified in three separate functions based on performance, and in the second phase, the results obtained in the laboratory regarding the amount of energy and light passing through the transparent polymeric samples (colored transparent filters (CTFs)) were imported into the software. Then, the optimization coding of each color for each month was written according to the ASHRAE standard. The months of summer and autumn spring were taken according to the geographic region. The percentage of the area for each transparent polymer was found to be more than the total area of the glass (if the shutters were taken vertically) for summer or autumn spring.

Using the MATLAB software program, the aim was to apply smart windows to the windows located in every direction of the building. Therefore, several functions have been determined in MATLAB, referred to as the City Function, Shading Function (refer to [49]), and Plan-Draw Function, respectively. In this study, the Plan-Draw Function has been discussed.

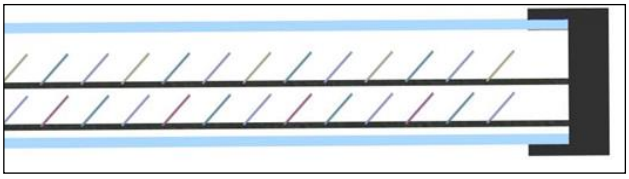

Figure 3. The plan view of suggested window

2.1. City Function

First of all, the climate is identified, and several cities of the world are already included. If the user cannot find the desired city, the excel climate data must be added to the Energy Plus site (https://energyplus.net/weather). The user transfers the climate conditions to the program by selecting the city.

2.2. Shading Function

Shading mode is a principal part of increasing energy efficiency. According to [50]: "Shaded areas on the radiation collecting solar aperture, however, may be useful or detrimental for the system, depending on its type and objective. The knowledge of light and shadow finds critical applications within solar architecture and urban planning". Typical action controls theoretical analyses of solar heat gain coefficient (SHGC) or energy-saving simulation of structures during a specified time for the shading behavior test [51]. As reported by [52], "the ability to compute the amount of shaded and unshaded area is required to evaluate the performance of a shading device based on the shadow cast on a window by the sunray."

In order to calculate the shading on a window plane, Jones rendered the shaded area by defining the vanguard edge components of the bump and the bottom of the window. This system was also applied for the content calculation of solar radiation on a vertical plate [53]. The trigonometric method is known to be the method that has been perused with considering the existence of awnings, parapets, and overhangs. Rectangular shapes that characterize their geometries are conformed to the geometry of shading on the parallel plane of the window and concurrent to its vertical axis [54].

The other method is SOMBRERO; as mentioned by [50]; "a PC-program written in Turbo-Pascal, calculates the GSC (geometrical shading coefficient), the proportion of the shaded area of an arbitrarily oriented surface surrounded by shading elements as a function of time end location." As introduced by [55], TRNSHD is another "PC-program which was developed for building simulations with TRNSYS. It is a stand-alone tool that is not restricted to either buildings or TRNSYS and thus can be used to solve other shading problems."

Another software tool was performed by [52], which uses Auto-CAD to graphically design the geometry of shading system and MATLAB to prepare the algorithmic simulations. Another MATLAB written program was developed by [56], which calculates the solar radiation and shadows on a rectangular surface. Based on [57]; "Quaschning and Hanitsch (1995) and Cascone et al. (2011) had presented methodologies in order to calculate the direct shading factor through the polygon projection method, and the diffuse shading factor through the radiance integration along the sky dome surfaces seen through a PV surface point". The system developed by Cascone et al. [2] is more complicated when compared to Quaschning and Hanitsch's method [58]. It was created using "MATLAB software tool," which inserts the exterior environment information from DXF files. Shading-Plus is another method which is used to calculate solar heat gain coefficient (SHGC) and this method is developed based on Energy-Plus (the computer simulation system) and uses its core simulation engine [51].

All of these research and simulation machines have details and advantages to be considered. However, all do not encompass all the fields to draw a suitable window system and shading form according to the plan and other criteria such as environmental elements. Therefore, a graphical program has been written in MATLAB program language to cope with this issue and solve research problems concerning shading with colored transparent filters (CTFs). In this program, the user must insert location, time, and other data withdrawing the plan of the project.

Solar Position

"The solar position concerning a point on the earth's surface can be determined by the solar azimuth angle φ and the solar elevation angle $\propto$. There are various methods to calculate the value of these parameters with geo-location data, date and time" [57, 59-61].

From Declination angle to Azimuth angle [62], all the developed algorithms and equations have been defined and used in this section.

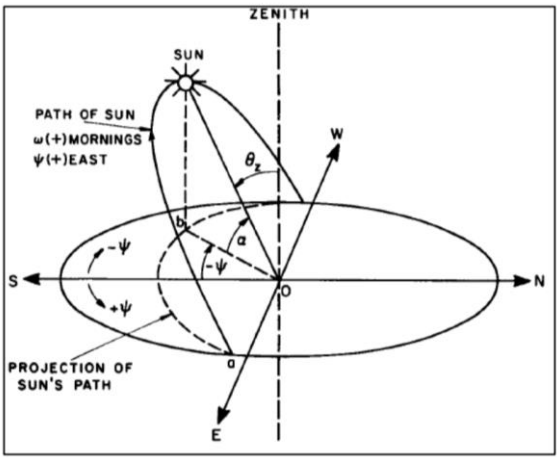

Figure 4. Sun's zenith, altitude, and azimuth angles [1]

Shadow Computation

Whenever the direct radiation does not have an impact on a surface, certainly there are shadows formed. The paper benefits from previous works conducted in order to compute the shadow of slabs or walls on the window, [2, 50-52, 56, 57, 63] and calculate the geometry of shadow on "Global Coordinate System XYZ" (the x-axis along the south direction, the y-axis along the east path and the z-axis along the zenith direction).

The Eq. (1) of a tilted plane through the origin is "ax + by + cz = 0", where the tilt plane will be our case study window surface, as seen in Figure 5.

$$e = \begin{cases} a = \cos\gamma \sin\varepsilon \\ b = \sin\gamma \cos\varepsilon \\ c = \cos\varepsilon \end{cases} \quad (1)$$

Where XY is the window surface coordinate system, and γ is the surface azimuth of the window plane (angle between south and -Y), and ε is the window surface (wall) tilt angle (normally 90°).

In order to set the solar vector in accordance with zone and time, S is found to be as Eq. (2)

$$S = \begin{cases} l = \cos\varphi \cos\propto \\ m = \sin A \cos\propto \\ n = \sin\propto \end{cases} \quad (2)$$

Where φ is solar azimuth angle and $\propto$ *is solar elevation angle.*

So, when e.s is negative, the sun is located at the back of the window surface to have a complete shadow, and when it is positive, the shadows of obstacles are formed.

The corner points with P0 (x0, y0, z0) are considered to determine the shadow of obstacles, and the following equations have been used to find P' (the shadow of P on window surface),

$$t = -\frac{ax_0+by_0+cz_0}{al+bm+cn} \quad (3)$$

$$P'\ (x'_0,\ y'_0,\ z'_0) = \begin{cases} x' = x_0 + l.t \\ y' = y_0 + m.t \\ z' = z_0 + n.t \end{cases} \quad (4)$$

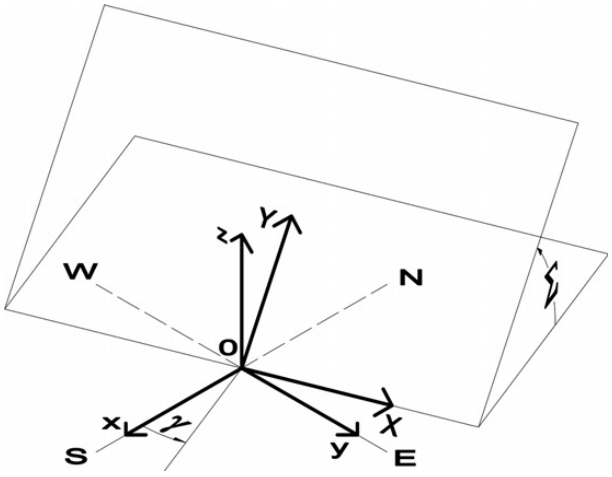

Figure 5. Window surface "Coordinate Systems" [2]

This needs to be turned to the x y plane because it is challenging to organize it in three dimensions. According to this, two matrixes are defined.

$$R_z(\tfrac{\pi}{2}+\gamma) = \begin{bmatrix} \sin\gamma & \cos\gamma & 0 \\ \cos\gamma & \sin\gamma & 0 \\ 0 & 0 & 1 \end{bmatrix} \quad (5)$$

$$R_x(\varepsilon) = \begin{bmatrix} 1 & 0 & 0 \\ 0 & \sin\varepsilon & -\sin\varepsilon \\ 0 & \sin\varepsilon & 1 \end{bmatrix} \quad (6)$$

The matrix (R_z) is assigned in Eq. (7) as follows:

$$R_z(\tfrac{\pi}{2}+\gamma) = \begin{bmatrix} -\sin\gamma & -\cos\gamma & 0 \\ \cos\gamma & -\sin\gamma & 0 \\ 0 & 0 & 1 \end{bmatrix} \quad (7)$$

To find P′ in the new XY coordinate system is found to be;

$$P'(X_0, Y_0) = (R_z . R_x) . P'\ (x'_0,\ y'_0, z'_0) \quad (8)$$

The shadow of the corner points of obstacles is formed and by connecting them, the geometry of shadow on the window surface is obtained.

The calculation of tree shadows and environment items is performed according to the Vegetation model [2]. A screenshot from the coding of the "Shading" function written in the MATLAB program can be seen in Figure 6.

```
HiR = SkyEmi * Sigma .* TempDry .^ 4;
LSTM = 15 * TimeZone;
B = 360 / 365 * (d - 81);
EoT = 9.87 * sind(2 * B) - 7.53 * cosd(B) - 1.5 * sind(B);
TC = 4 * (Lon - LSTM) + EoT;
LST = HourM + TC / 60;
HRA = 15 * (LST - 12);
DeclinationAng = 23.45 * sind(B);
SunR = 12 - acosd(-tand(Lat) .* tand(DeclinationAng)) / 15;
SunS = 12 + acosd(-tand(Lat) .* tand(DeclinationAng)) / 15;
RandS = (HourM > SunR) .* (HourM < SunS);
ElevationAng = asind(sind(DeclinationAng) .* sind(Lat) + ...
    cosd(DeclinationAng) .* cosd(Lat) .* cosd(HRA)).* RandS;
RandS(RandS == 0) = NaN;
AzimuthAng = acosd((sind(DeclinationAng) .* cosd(Lat) - ...
    cosd(DeclinationAng) .* sind(Lat) .* cosd(HRA)) ./ ...
    cosd(ElevationAng)).* RandS;
% ---------------------------------------------------
load('TestData');
% --------- l,m,n ------------------------
s.l = cosd(AzimuthAng) .* cosd(ElevationAng);
s.m = sind(AzimuthAng) .* cosd(ElevationAng);
s.n = sind(ElevationAng);
% --------- P calculation ----------------------
% P = cell([2 * U.SlabNum + length(U.OutsideWall) 2]);
% for j = 1 : 2 : 2 * U.SlabNum
%     P{j,1} = cat(1, U.AwningSlab{j}, repmat(U.SlabGH(j),1,...
%         size(U.AwningSlab{j},2)));
%     P{j + 1,1} = cat(1, U.AwningSlab{j}, repmat(U.SlabGH(j) + U.SlabH(j),1,...
%         size(U.AwningSlab{j},2)));
% end
j = -1;
for i = 1 : length(U.OutsideWall)
    P{i + j + 1,1} = cat(1, U.OutsideWall{i}, repmat(U.ZoneGH + ...
```

Figure 6. A screenshot from the "Shading" function, MATLAB program

2.3. Plan-Draw Function

The "Plan-Draw" function is defined to find the window's position relative to the building and the building's environment. The Plan-Draw function allows the user to quickly enter window, zone, wall, and shading data in two dimensions. For the user to enter the building data, this function is described in the MATLAB program, and then its codes are entered. Then, two-dimensional drawings and position data are combined in three-dimensional matrices. The icons used in this program, and the selection of the required data are taken from the ArchiCAD program. According to this function, a user must draw the zone plans one by one and ensure that the necessary data are entered. According to this function, after drawing the zone by a user, the exterior walls, shading, and windows must be drawn to determine the criteria. The schemes of the drawing part of the software tool have been shown in Figure 7.

The window position (x, y, z) is defined after entering the height of the window and its height from the floor. Shadowing on windows is explained as time and geometry according to solar azimuth and solar elevation angle. After this step, the shadowing is simulated daily according to the plan of the user.

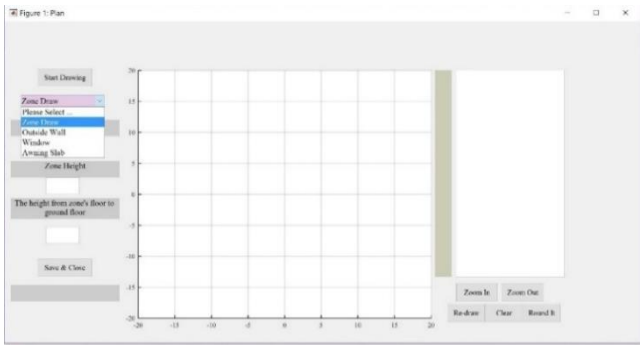

Figure 7. Ready to draw; Plan-Draw function of software tool written in MATLAB program

4. Results and Discussion

The amount of energy and light passing through the color samples were obtained and entered into the designed software. In this regard, specimens in the laboratory were tested by two types of spectrophotometer devices. The BECKMEN DU 530 spectrophotometer was used to measure the transmission of light through the visible and infrared wavelengths, and the FT-IR spectrophotometer was used to measure the transmission of light through ultraviolet wavelengths for each of the six colors of transparent polymer specimens. In each of the transparent colored samples of CTFs, the percentage of passing light compared to the wavelength and the required calculations of the amount of energy and brightness passing through each of the translucent polymers were achieved by obtaining a graph.

4.1. Thermal Radiation

The spectrum of electromagnetic radiation encompasses y rays, x rays, ultraviolet radiation, light, heat, radio waves, and radar waves. Electromagnetic radiation is generally classified by wavelength, though frequency and wavenumber are also used. Frequency (v), as shown in Eq. (9), has the advantage over a wavelength because it does not change when radiation passes from one medium to another [64]:

$$\text{Frequency (V)} = C0 \,/\, \lambda vac \qquad (9)$$

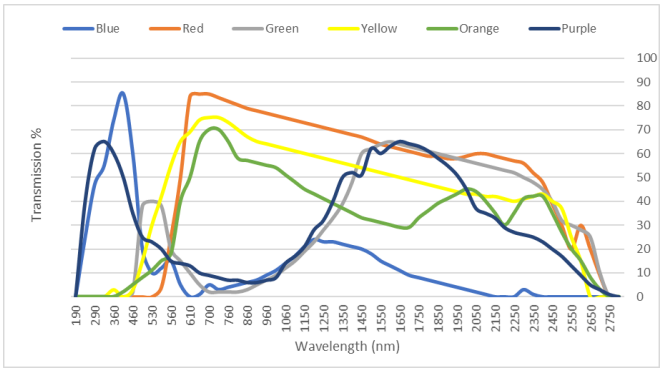

Figure 8. Transmission spectra by CTF's color in the wavelength range between 190nm and 3000 nm

*Where C0 is the speed of propagation for electromagnetic radiation in a vacuum (C0 = 2.998 * 108 m/sec) and λ is wavelength.*

So, the spectrally integrated direct irradiance on a surface normal to the sunrays (also called direct normal radiation) and at a mean sun-earth distance is given as Eq. (10) [65]:

$$I_n = \sum_{\lambda=0}^{\infty} I_{0n\lambda}\, \tau_\lambda\, \Delta\lambda \qquad (10)$$

Colored filters were placed in the bathtub with glass in such a way to be closer to the actual conditions in the lab work. The sample was prevented from moving in the bathtub, and the spectrum was obtained vertically. Typically, certain conditions could occur since the liquid was put into the bathtub; but since the samples were solid, it was necessary to pay attention to how they were placed, keep them clean and suitable for the full bathtub size.

UV-VIS wavelength transmittance was calculated by BECKMEN DU 530 Spectrophotometer with a wavelength range of 190-1100 nm. Near-Infrared wavelength

transmittance was calculated by GL-6021 Galaxy Series FT-IR Spectrometer with Infrared MIO465-0053-03 having a wavelength range of 1100-3000 nm. The transition percentage of the two devices was combined in the range of UV-VIS-IR wavelengths, and the calculations were carried out via MATLAB. These two devices cover wavelengths of 190-3000nm. Different spectrophotometers should be used for longer ultraviolet wavelengths, which are not necessary while mitigating the solar radiations (Figure 8).

After achieving the transmission spectra of each color of CTFs, the thermal and lighting transmittance of CTF will be defined. So, for thermal transmission, we have the following integral formulations:

If there is an angular dependence of τ_λ, the total transmittance at angle θ can be written as shown in Eq. (11) [66]:

$$\tau(\theta) = \frac{\int_0^\infty \tau_\lambda(\theta)\, I_{\lambda i}(\theta)\, d\lambda}{\int_0^\infty I_{\lambda i}(\theta)\, d\lambda} \quad (11)$$

According to [66], "In a multi-cover" system in which the covers have significant wavelength-dependent properties, the spectral distribution of the solar radiation changes as it passes through each surface."

And according to this point, as shown in Eq. (11) by [66]: "at any wavelength λ, the transmittance is the product of the monochromatic transmittances of the individual covers." Therefore, for N covers (N is 3 or 4 covers in this study) the formula can be written as Eq. (12)

$$\tau\,\alpha(\theta) = \frac{\int_0^\infty \tau_{\lambda,1}(\theta)\,\tau_{\lambda,2}(\theta)\ldots\,\tau_{\lambda,n}(\theta)\;\alpha_\lambda(\theta)\, I_{\lambda i}(\theta)\, d\lambda}{\int_0^\infty I_{\lambda i}(\theta)\, d\lambda} \quad (12)$$

After completing the drawings regarding zone and other parameters, the program can simulate direct incident and diffused beam radiation.

"The incident global solar radiation (I) received by a surface, such as a window, is a combination of direct beam radiation (Ib), sky radiation (Is), and radiation reflected from the ground in front of the surface (Ir)" [67]:

$$\boldsymbol{I = I_b\, cos(\theta) + I_s + I_t} \quad (13)$$

θ is the incident angle of the sunrays incident to the surface.

$$I_s = I_{dh}\,[0.5\,(1 - F_1)(1 + cos\beta) + F_1\, a/b + F_2 sin\,\beta] \quad (14)$$

Where

"I_{dh} = diffused solar horizontal radiation

F_1= circumsolar anisotropy coefficient, the function of sky condition

F_2= horizon/zenith anisotropy coefficient, the role of sky condition

θ = tilt of the surface from the horizontal

a = 0 or the cosine of the incident angle, whichever is greater

b = 0.087 or the cosine of the solar zenith angle, whichever is greater".

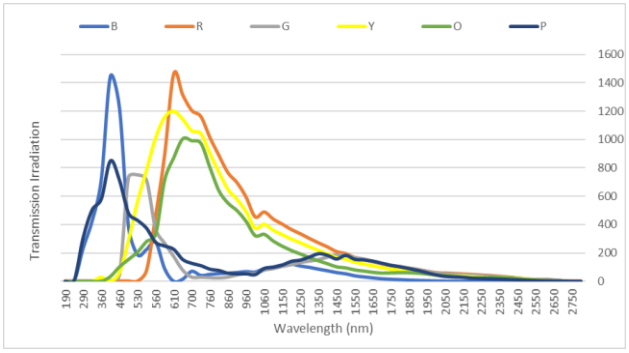

Figure 9. Transmittance irradiation by CTFs in the wavelength range of 190- 3000 nm

"The ground-reflected radiation (I_t) received by a surface is assumed to be isotropic and is a function of the global horizontal radiation (I_b), the tilt of the surface from the horizontal (β), and the ground reflectivity or albedo (ρ)" [67]:

$$I_t = 0.5\rho I_b\,(1 - cos\,(\beta)) \quad (15)$$

If we ignore the shadow of sky radiation and reflected radiation from the ground, we can obtain the Eq. (16) for the energy received by the window glass.

$$I_w = (A - A_s)\, I_b\, cos(\theta) + A\, I_s + A\, I_t \quad (16)$$

Where A is the glazing area, and A_s is the shading area of window glass.

After coding all the necessary equations in MATLAB, two diagrams of "Solar Radiation Spectrum Sea Level" and "Transmission Spectra from CTFs" can be multiplied by each other. Figure 9 shows the multiplied diagram of transmission and radiation in the wavelength range of 190 to 3000 nm.

Transmittance irradiation by colors can be seen in Figure 9, which is the multiplication of each color's transmittance to solar radiation in the wavelength range of 190- 3000 nm.

So, according to the equations, the transmittance irradiation of CTFs at a right angle of 90º has been calculated in Table 1 as follows:

Table 1. Transmittance irradiation of CTFs and Transmittance Irradiation of CTFs per Solar Irradiance

	Blue	Red	Green	Yellow	Orange	Purple
Transmittance Irradiation	296042.6	662585.8	296847.7	616126.4	474173.4	356262.5
Transmittance Irradiation/ Solar Irradiation	0.221444	0.495623	0.222046	0.460871	0.354688	0.266489

When compared to other colors, red and yellow samples are found to have transmitted the highest amount of solar irradiation and blue, purple, and green ones are found to have transmitted the lowest amount of irradiation transmittance.

4.2. Light Transmission

According to the diagram of light passing percentage through the devices considering the corresponding equation, the light transmission level of each color becomes accessible to each other.

As stated in the obtained graphs of transmission spectra of CTFs, the percentage of light passing through two devices for each of the colors has been investigated.

"The light transmittance of the composite was measured at a wavelength ranging from 200 to 1100 nm using a transmission optical spectrometer" [68].

Transmission spectra of CTFs by wavelengths between 360-710 nm drawn using MATLAB can be seen in Figure 10, where the grey graph shows the sensitivity of the human eye. In order to calculate the ratio of light transmission of CTFs to each other, Eq. (17) can be used as:

$$Lum\ Lamda(i) = \frac{\int_{min\,\lambda i,\,\lambda p}^{max\,\lambda i,\,\lambda p} \tau_\lambda}{\int \tau_{\lambda p}} \quad (17)$$

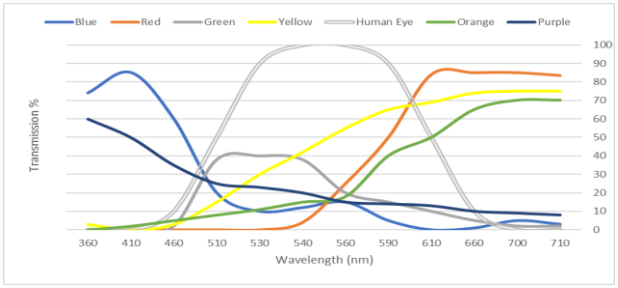

Figure 10. Transmission Irradiation of CTFs based on whether or not the sensitivity of the human eye is the same for different visible wavelengths.

Luminance transmittance of CTFs can be seen in the second row of Table 2 as a proportion ratio to the human eye sensitivity. Yellow and purple have the most lighting transmittance in comparison with other colors.

Table 2. Light transmission of CTFs

	Blue	Red	Green	Yellow	Orange	Purple
$\int_{400}^{700} \tau_\lambda$	4055	3300	3775	5320	3170	4950
Lum Lamda (400-700)	0.347323	0.282655	0.32334	0.455675	0.27152	0.423983

4.3. Optimization and System Outputs of Windows

Computer programs have been written according to climate and sunlight data to describe the Smart Window Designed Tool (SWDT), considering the position of the windows and their surroundings. The program is limited to two season types (spring-autumn and summer) and presents the panes' areas and numbers according to the panes' transmission wavelengths. It then allows each window to move according to the daily sun position and its exposure using the sensors.

World map of the "Köppen- Geiger climate classification" updated as supplemental material on the internet at "http://koeppen-geiger.vu-wien.ac.at/" have been used to determine the two suggested seasons of summer and spring-autumn in the program (Figure 11).

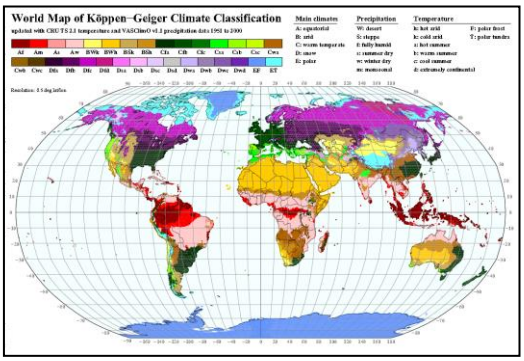

Figure 11. World Map of the "Köppen- Geiger" climate classification updated [69]

Climate and their season classifications placed in the northern and southern hemispheres have been shown in Table 3.

Table 3. A and B Climate classifications and seasons

Climates	Summer	Spring/Autumn
A (Northern)	May, June, July, August	December, January
A (Southern)	November, December January, February	June, July
B (Northern)	May, June, July	August, September October, March, April
B (Southern)	November, December, January, February	March, April, September, October
C (Northern)	June, July, August	September, October November, March April, May
C (Southern)	December, January February	March, April, May, September, October November
D	June, July, August	September, October April, May

Samples in rainy climates can be eliminated from the test.

According to [70];

"In the summer, the coordinates are:

T_o = 22.6-26.0°C at 16.7°C T_{dp} and T_o= 23.3-27.2°C at 1.7°C. T_{dp}."

The sloped sides are defined by [71];

"ET = 22.8°C and 26.1°C. The Maximum limit for mean air velocity in the winter is 0.15 m/s. In the summer, the limit is nominally 0.25 m/s, increasing an additional 0.275 m/s for each °C above 26°C dry-bulb temperature, up to a maximum of 0.8 m/s for temperatures above 28°C."

Conforming to [70];

"In the winter, operative temperature and humidity limits are defined by a comfort zone on the psychrometric chart having the following coordinates:

T_o = 19.5-23.0°C at 16.7°C T_{dp} and T_o = 20.2-24.6 C at 1.7°C T_{dp}."

The sloped sides are defined by [72] ;

"The new effective temperature is denoted by ET. The winter limits are found to be ET= 20.0 °C and 23.6 °C, respectively."

As reported by [71]; "The following conditions define no uniformity limits: the vertical air temperature difference between the 0.1 and 1.7 m heights shall not exceed 3°C; radiant temperature asymmetry in the vertical direction shall be less than 5°C and in the horizontal direction less than 10°C; and the floor surface temperature shall be between 18°C and 29°C".

The evaluation, calculation, and finding of the optimum of two charts in terms of solar radiant and lighting according to the season in the zone have been carried out in this part. The multi-objective optimization function has been written in MATLAB (as shown in Figure 12) to find the case of colors and their area percentage. The last function has been introduced based on irradiation and lighting transmittance of CTFs. The cooling load and irradiation transmission must be minimal and the lighting transmittance must be maximal.

est.m | OptFun.m

```
function Obj = OptFun(guess,QLamda,LumLamda,QT)
a = guess(1);
b = guess(2);
c = guess(3);
d = guess(4);
obj1 = sum([a b c d] .* LumLamda) -.6;
obj2 = sum([a b c d] .* QLamda(1:4))-QT;
obj3 = sum([a b c d]) - 1;
Obj = obj1 ^ 2 + obj2 ^ 2 + obj3 ^ 2;
end
```

Figure 12. A screenshot from "Optimization" function

5. Conclusion

The smart window is considered as mid-pane shading with horizontal shutters, and the SWDT was developed to respond to its system. Therefore, if the direction of shutters changes horizontally or in other patterns, color compositions should be considered. The SWDT has been evaluated and verified as shown in the diagrams and simulation charts and their comparisons. However, the space percent of colors is determined in the program with a drawing zone plan by a user conforming to all data climate and incident solar radiation and daylighting. The SWDT designed to be used by architects can also be an energy sustainability tool for ease of design by considering the brightness and optimal heating of solar radiant energy.

The results show that:

- The blue and green transparent filters have 22% transmittance irradiation with 34% and 32% daylight transmission, respectively. Therefore, the expectations are to have more percentages in buildings developed in A climate classification.
- The materials used and the shutter system applied in the proposed window seem to be economical considering the color of the CTF in the case of significant production. It can be an excellent alternative to current windows, confirming reduced cooling load and lighting.
- The color percentages calculated based on the zone, climate, position, and the given window size data will – by the recognized method – be able to provide designers with an opportunity to create different compositions by providing indoor comfort conditions in the context of thermal and lighting without needing test potential on the facades nor other shading elements.

In this study, all irradiance formulas have been entered in smart window design and computer program with prerequisites. In this study, the effect of factors such as glass type and material were not considered. Therefore, further studies are recommended to collect such data to improve forecasting performance. The material properties can be examined for future works, and nanomaterials can be tested literally for this issue. The pattern of colors can be analyzed, and the collection of them for a better response of energy efficiency may be tested. The design, direction, and geometry composition of used colors can be analyzed due to the window position, shading elements, and the other considered properties, and the effect of this alteration on lighting and energy consumption can be calculated. The impact of the closed jalousies (vertical blinds) in winter and cold nights can be calculated to find out their positive or negative effects on reducing the heating load in future works. And finally, the psychological aspects of the effects of windows on users in different spaces with different land uses can be analyzed in future works.

References

[1] M. Iqbal, Sun-Earth Astronomical Relationships, 1983.

[2] Y. Cascone, V. Corrado, V. Serra, Calculation procedure of the shading factor under complex boundary conditions, Solar Energy 85(10) (2011) 2524–2539.

[3] M. Haghshenas, M.R. Bemanian, Z. Ghiabaklou, Analysis of the photo–damaging performance of persian "orosi" in carpeted and non–carpeted spaces, İran Bilim ve Teknoloji Üniversitesi 25(2) (2015) 94–99.

[4] L. Pérez-Lombard, J. Ortiz, C. Pout, A review on buildings energy consumption information, Energy and buildings 40(3) (2008) 394–398.

[5] D. Fiaschi, R. Bandinelli, S. Conti, A case study for energy issues of public buildings and utilities in a small municipality: Investigation of possible improvements and integration with renewables, Applied energy 97 (2012) 101–114.

[6] L. Yang, H. Yan, J.C. Lam, Thermal comfort and building energy consumption implications – A review, Applied Energy 115 (2014) 164–173. https://doi.org/https://doi.org/10.1016/j.apenergy.2013.10.062.

[7] L. Yang, J.C. Lam, C.L. Tsang, Energy performance of building envelopes in different climate zones in China, Applied Energy 85 (2008) 800–817.

[8] M. Bojic, F. Yik, K. Wan, J. Burnett, Influence of envelope and partition characteristics on the space cooling of high-rise residential buildings in Hong Kong, Building and Environment 37 (2002) 347–355.

[9] M.A.A.E.D. Ahmed, M.A. Fikry, Impact of glass facades on internal environment of buildings in hot arid zone, Alexandria Engineering Journal 58(3) (2019) 1063–1075.

[10] M.T. Ercan, M.T. Kayili, B.S. Qurraie, The Effects of Green Roof on Heat Loss and Energy Consumption in the Buildings, Computational Research Progress in Applied Science & Engineering 07 (2021).
[11] R. Stair, C.A. Faick, Infrared absorption spectra of some experimental glasses containing rare earth and other oxides, J. Res. Natl. Bur. Stand.(1934) 38(Jan) (1947) 95-101.
[12] A.T. Giese, C.S. French, The analysis of overlapping spectral absorption bands by derivative spectrophotometry, Applied spectroscopy 9(2) (1955) 78–96.
[13] R. Mitchell, C. Kohler, D. Arasteh, THERM 5.2/WINDOW 5.2 NFRC Simulation Manual, Lawrence Berke-ley National Laboratory, University of California, Berkeley, CA (2006).
[14] L. V. Besteiro, X.-T. Kong, Z. Wang, F. Rosei, A.O. Govorov, Plasmonic glasses and films based on alternative inexpensive materials for blocking infrared radiation, Nano letters 18 (2018) 3147–3156.
[15] P. France, Fluoride glass optical fibres, Springer Science & Business Media2012.
[16] G. Alvarez, J. Flores, J. Aguilar, O. Gómez-Daza, C. Estrada, M. Nair, P. Nair, Spectrally selective laminated glazing consisting of solar control and heat mirror coated glass: preparation, characterization and modelling of heat transfer, Solar Energy 78 (2005) 113–124.
[17] N. Vigener, M. Brown, Building Envelope Design Guide–Glazing, Whole Building Design Guide, National Institute of Building Science (2009).
[18] J. Savić, D. Đurić-Mijović, V. Bogdanović, Architectural glass: Types, performance and legislation, Facta universitatis-series: Architecture and Civil Engineering 11 (2013) 35–45.
[19] S. Somasundaram, A. Chong, Z. Wei, S.R. Thangavelu, Energy saving potential of low-e coating based retrofit double glazing for tropical climate, Energy and Buildings 206 (2020) 109570.
[20] C. Sol, J. Schläfer, I.P. Parkin, I. Papakonstantinou, Mitigation of hysteresis due to a pseudo-photochromic effect in thermochromic smart window coatings, Scientific reports 8 (2018) 1–6.
[21] N.K. Kapur, A comparative analysis of the radiant effect of external sunshades on glass surface temperatures, Solar Energy 77 (2004) 407–419.
[22] N. Abundiz-Cisneros, R. Sanginés, R. Rodríguez-López, M. Peralta-Arriola, J. Cruz, R. Machorro, Novel Low-E filter for architectural glass pane, Energy and Buildings 206 (2020) 109558.
[23] A.M. Yousef Gorji, Orosi, A Tool for Controlling Daylight (Case of Study: Qajar dynasty Houses of Qazvin), Scientific and Research Journal of The Scientific Society of Architecture & Urbanism 8 (2017) 225–236.
[24] Z.S.A. Mehrizi, M. Marasy, The Comparative Study of Art of Manufacturing Orosi and Stained Glass Windows in Iran and Europe, Journal of History Culture and Art Research 6 (2017) 233–243.
[25] S.N. Hosseini, S.M. Hosseini, M. HeiraniPour, The Role of Orosi's Islamic Geometric Patterns in the Building Façade Design for Improving Occupants' Daylight Performance, Journal of Daylighting 7 (2020) 201–221.
[26] M. Haghshenas, Z. Ghiyabaklu, The effect of colored glass on the light and energy transmission in the visible region, (2006).
[27] F. Pacheco-Torgal, J. Labrincha, L. Cabeza, C.G. Granqvist, Eco-efficient materials for mitigating building cooling needs: design, properties and applications, Woodhead Publishing2015.
[28] J.A. Duffie, W.A. Beckman, N. Blair, Solar engineering of thermal processes, photovoltaics and wind, John Wiley & Sons2020.
[29] F. Allard, M. Santamouris, Natural Ventilation in Buildings: A Design Handbook (BEST (Buildings, Energy and Solar Technology), Publisher: Routledge (2002).
[30] A.K. Chowdhary, D. Sikdar, Design of electrotunable all-weather smart windows, Solar Energy Materials and Solar Cells 222 (2021) 110921.
[31] R. Zakirullin, Chromogenic materials in smart windows for angular-selective filtering of solar radiation, Materials Today Energy 17 (2020) 100476.
[32] J. Pan, R. Zheng, Y. Wang, X. Ye, Z. Wan, C. Jia, X. Weng, J. Xie, L. Deng, A high-performance electrochromic device assembled with hexagonal WO3 and NiO/PB composite nanosheet electrodes towards energy storage smart window, Solar Energy Materials and Solar Cells 207 (2020) 110337.
[33] A. Llordés, G. Garcia, J. Gazquez, D.J. Milliron, Tunable near-infrared and visible-light transmittance in nanocrystal-in-glass composites, Nature 500 (2013) 323–326.
[34] S. Haghanifar, T. Gao, R.T.R. De Vecchis, B. Pafchek, T.D. Jacobs, P.W. Leu, Ultrahigh-transparency, ultrahigh-haze nanograss glass with fluid-induced switchable haze, Optica 4 (2017) 1522–1525.
[35] B. Wang, M. Cui, Y. Gao, F. Jiang, W. Du, F. Gao, L. Kang, C. Zhi, H. Luo, A Long-Life Battery-Type Electrochromic Window with Remarkable Energy Storage Ability, Solar RRL 4 (2020) 1900425.
[36] A. Abdel-Moneim, M. AbdelKader, USING SMART MATERIALS IN SMART WINDOWS FOR ENERGY EFFICIENCY OF BUILDINGS, Journal of Al-Azhar University Engineering Sector 17 (2022) 345–354.
[37] A. Hedge, D. Nou, Worker reactions to electrochromic and low e glass office windows, Ergonomics International Journal 2 (2018).
[38] C.B. Moler, Numerical computing with MATLAB, SIAM2004.
[39] I. Sahraei, A. Jalili, H.A. Bagal, The Effect of Demand Response in Improvement Solar manufacturers Profit Connected to Grid in Deregulated Power Market, Computational Research Progress in Applied Science & Engineering 03 (2017).
[40] M. Abbasi, Simultaneous Power Network Reconfiguration and DG Allocation Using Improved Jaya Algorithm for Maximum Loadability Improvement and Power Loss Reduction, Computational Research Progress in Applied Science & Engineering 07 (2021).
[41] B.S. QURRAIE, PROVIDING OPTIMUM LIGHTING AND REDUCING HEAT GAIN THROUGH INVESTIGATION OF DIFFERENT WAVELENGTH EFFECT OF COLORS IN TRANSPARENT FACADES: SMART WINDOW DESIGN TOOL, (2019).
[42] Y. Zhang, L. Huang, Y. Zhou, Analysis of indoor thermal comfort of test model building installing double-glazed window with curtains based on CFD, Procedia Engineering 121 (2015) 1990–1997.
[43] G. Weir, T. Muneer, Energy and environmental impact analysis of double-glazed windows, Energy Conversion and Management 39 (1998) 243–256.
[44] R. Southall, M. McEvoy, Results from a validated CFD simulation of a supply air 'ventilated'window, RoomVent 2000-7th International Conference on Air Distribution in Rooms, 2000.
[45] T. Chow, K. Fong, W. He, Z. Lin, A. Chan, Performance evaluation of a PV ventilated window applying to office building of Hong Kong, Energy and Buildings 39 (2007) 643–650.
[46] C. Zhang, W. Gang, J. Wang, X. Xu, Q. Du, Experimental investigation and dynamic modeling of a triple-glazed exhaust air window with built-in venetian blinds in the cooling season, Applied Thermal Engineering 140 (2018) 73–85.

[47] F. Gloriant, P. Tittelein, A. Joulin, S. Lassue, Modeling a triple-glazed supply-air window, Building and Environment 84 (2015) 1–9.
[48] C. Zhang, W. Gang, J. Wang, X. Xu, Q. Du, Numerical and experimental study on the thermal performance improvement of a triple glazed window by utilizing low-grade exhaust air, Energy 167 (2019) 1132–1143.
[49] B.S. Qurraie, F. Beyhan, Using a Shading Tool to Reform Window designing due to Solar Radiation, IJARE 4 (2018) 1.
[50] A. Niewienda, F. Heidt, SOMBRERO: A PC-tool to calculate shadows on arbitrarily oriented surfaces, Solar Energy 58 (1996) 253–263.
[51] Y. Ye, P. Xu, H. Sha, P. Yue, H. Zhang, ShadingPlus—a fast simulation tool for building shading analysis, Energy Efficiency 9 (2016) 239–248.
[52] C. Pongpattana, P. Rakkwamsuk, Efficient algorithm and computing tool for shading calculation, Songklanakarin Journal of Science and Technology 28(2) (2006) 375–386.
[53] R. Yanda, R. Jones, Shading effects of finite width overhang on windows facing toward the equator, Solar Energy 30 (1983) 171–180.
[54] R. Bekooy, Computer shadow analysis technique for tilted windows shaded by overhangs, vertical projections, and side fins, ASHRAE Trans.;(United States) 89(1A) (1983).
[55] M.D. Hiller, W.A. Beckman, J.W. Mitchell, TRNSHD—a program for shading and insolation calculations, Building and Environment 35 (2000) 633–644.
[56] B. Keller, A. Costa, A Matlab GUI for calculating the solar radiation and shading of surfaces on the earth, Computer Applications in Engineering Education 19 (2011) 161–170.
[57] E.G. Melo, M.P. Almeida, R. Zilles, J.A. Grimoni, Using a shading matrix to estimate the shading factor and the irradiation in a three-dimensional model of a receiving surface in an urban environment, Solar Energy 92 (2013) 15–25.
[58] V. Quaschning, R. Hanitsch, Numerical simulation of photovoltaic generators with shaded cells, simulation 2 (1995) 6.
[59] J.J. Michalsky, The astronomical almanac's algorithm for approximate solar position (1950–2050), Solar energy 40 (1988) 227–235.
[60] M. Blanco-Muriel, D.C. Alarcón-Padilla, T. López-Moratalla, M. Lara-Coira, Computing the solar vector, Solar Energy 70(5) (2001) 431–441.
[61] I. Reda, A. Andreas, Solar position algorithm for solar radiation applications, Solar energy 76(5) (2004) 577–589.
[62] ASHRAE, Handbook of Fundamentals, American Society of Heating, Air Conditioning, and Refrigerating Engineers , Inc., Atlanta, 2009.
[63] M.D. Hiller, TRNSHD-A Program for Shading and Insolation Calculations, University of Wisconsin-Madison, 1996.
[64] M. Günther, N. Janotte, A. Mezrhab, K. Pottler, C. Schillings, S. Wilbert, F. Wolferstätter, Solar radiation, Advanced CSP Teaching Materials, Enermena (2011) 22–23.
[65] L. Wald, BASICS IN SOLAR RADIATION AT EARTH SURFACE, (2018).
[66] J.A. Duffie, W.A. Beckman, Solar engineering of thermal processes, John Wiley & Sons2013.
[67] R. Perez, P. Ineichen, R. Seals, J. Michalsky, R. Stewart, Modeling daylight availability and irradiance components from direct and global irradiance, Solar energy 44 (1990) 271–289.
[68] H. Sato, H. Iba, T. Naganuma, Y. Kagawa, Effects of the difference between the refractive indices of constituent materials on the light transmittance of glass-particle-dispersed epoxy-matrix optical composites, Philosophical Magazine B 82 (2002) 1369–1386.
[69] M. Kottek, J. Grieser, C. Beck, B. Rudolf, F. Rubel, World map of the Köppen-Geiger climate classification updated, Meteorologische Zeitschrift 15 (2006) 259–263.
[70] ASHRAE, Handbook of Fundamentals, ASHRAE Standard 55, Thermal environmental conditions for human occupancy, American Society of Heating, Air Conditioning, and Refrigerating Engineers , Inc., Atlanta, 1981.
[71] ASHRAE, ASHRAE Handbook-Fundamentals, F09 -- THERMAL COMFORT (SI), American Society of Heating, Air Conditioning and Refrigerating Engineers, Inc., Atlanta, 2017.
[72] A. ASHRAE, ASHRAE. Thermal Environmental Conditions for Human Occupancy; Addendum h to ANSI/ASHRAE Standard 55-2010, American Society of Heating, Refrigerating and Air Conditioning Engineers, Inc.: Atlanta, GA, USA (2013).